CDFS-6664: A Candidate of Lyman-continuum Emission at $z \sim 3.8$ Detected by the Hubble Deep UV Legacy Survey

Fang-Ting Yuan[1] ⓘ, Zhen-Ya Zheng[1] ⓘ, Ruqiu Lin[1,2], Shuairu Zhu[1,2], and P. T. Rahna[1] ⓘ

[1] Key Laboratory for Research in Galaxies and Cosmology, Shanghai Astronomical Observatory, Chinese Academy of Sciences, 80 Nandan Road, Shanghai 200030, People's Republic of China; yuanft@shao.ac.cn

[2] University of Chinese Academy of Sciences, No. 19A Yuquan Road, Beijing 100049, People's Republic of China

Abstract

We report the detection of Lyman continuum (LyC) emission from the galaxy, CDFS-6664, at $z = 3.797$ in a sample of Lyman break galaxies with detected [O III] emission lines. The LyC emission is detected with a significance $\sim 5\sigma$ in the F336W band of the Hubble Deep UV Legacy Survey, corresponding to the 650–770 Å rest frame. The light centroid of the LyC emission is offset from the galaxy center by about $0\rlap{.}''2$ (1.4 pkpc). The Hubble deep images at longer wavelengths show that the emission is unlikely provided by low-redshift interlopers. The photometric and spectroscopic data show that the possible contribution of an active galactic nucleus is quite low. Fitting the spectral energy distribution of this source to stellar population synthesis models, we find that the galaxy is young (~ 50 Myr) and actively forming stars with a rate of $52.1 \pm 4.9\,M_\odot\,\mathrm{yr}^{-1}$. The significant star formation and the spatially offset LyC emission support a scenario where the ionizing photons escape from the low-density cavities in the ISM excavated by massive young stars. From the nebular model, we estimate the escape fraction of LyC photons to be $38\% \pm 7\%$ and the corresponding intergalactic medium (IGM) transmission to be 60%, which deviates more than 3σ from the average transmission. The unusually high IGM transmission of LyC photons in CDFS-6664 may be related to a foreground type-2 quasar, CDF-202, at $z = 3.7$, with a projected separation of $1\rlap{.}'2$ only. The quasar may have photoevaporated optically thick absorbers and enhance the transmission on the sightline of CDFS-6664.

Unified Astronomy Thesaurus concepts: High-redshift galaxies (734); Reionization (1383)

1. Introduction

During the epoch of reionization, the neutral and opaque intergalactic medium (IGM) transforms to ionized and transparent. The process requires Lyman continuum (LyC, $h\nu > 1$ Ryd) photons that can ionize the neutral hydrogen gas. Currently, the nature and properties of the sources of the reionization are still in debate. The two sources generally accepted to keep the IGM ionized are quasars and star-forming galaxies, but the relative contribution of these sources and their dependence on the cosmic time are still not clear (e.g., Madau & Dickinson 2014; Dayal et al. 2020). Previous works find that the number density of quasars may decline rapidly at $z > 3$ (e.g., Hopkins et al. 2007). Therefore, star-forming galaxies may be the main source of the LyC photons at high redshift (e.g., Steidel et al. 2001).

The ability of LyC photons from galaxies to ionize the IGM depends on how many of the ionizing photons can escape from the galaxy environment considering the absorption of the interstellar gas and dust, that is, the escape fraction of the LyC photons (f_{esc}). However, there is still a lack of knowledge about the average escape fraction from the star-forming galaxy population (e.g., Grazian et al. 2017).

The most straightforward method to measure f_{esc} is to detect LyC photons from galaxies directly. In recent years, several works have detected LyC sources from the nearby universe to redshift ~ 4 (e.g., de Barros et al. 2016; Shapley et al. 2016; Vanzella et al. 2016; Bian et al. 2017; Izotov et al. 2018;

Fletcher et al. 2019; Nakajima et al. 2020; Saha et al. 2020). However, the success rate of searches of LyC emitters at high redshift is still quite low. The detection of distant LyC sources is difficult for the following reasons. (1) Contamination from foreground sources can produce false LyC detections. (2) LyC visibility is quite stochastic because of the stochastic character of the IGM transmission; the irregular geometrical distribution of gas, dust, and stars in galaxies; and the short f_{esc} duty cycle over cosmic time. (3) Current facilities only allow us to probe LyC from relatively luminous galaxies, which intrinsically have a lower escape fraction of photons (Inoue & Iwata 2008; Mostardi et al. 2015; Siana et al. 2015; Vanzella et al. 2016). As a result, there are only a few LyC emitters that have been detected at $z > 3$, although these galaxies are crucial for us to understand the mechanism that allows ionizing photons to escape.

As the accumulation of observations grows, the chance of detecting LyC sources also increases. Deep and large surveys enable us to find more LyC sources. Researchers also find that galaxies with certain features are more likely to be LyC emitters. Lyα lines, [O III]/[O II] ratios, and ultraviolet (UV) absorption lines are useful probes to select LyC emitter candidates (e.g., Heckman et al. 2011; Jaskot & Oey 2014; Nakajima & Ouchi 2014; Alexandroff et al. 2015; Verhamme et al. 2015; Dayal & Ferrara 2018; Nakajima et al. 2020). These pre-selection methods further increase the detection rate of LyC emitters.

In this work, we report a detection of LyC emission arising from an emission line galaxy at $z = 3.797$ based on Hubble Space Telescope (HST) observations. The photometric and spectroscopic data of this object enable us to make a detailed analysis of its properties. Throughout this paper, we use pkpc and pMpc (ckpc
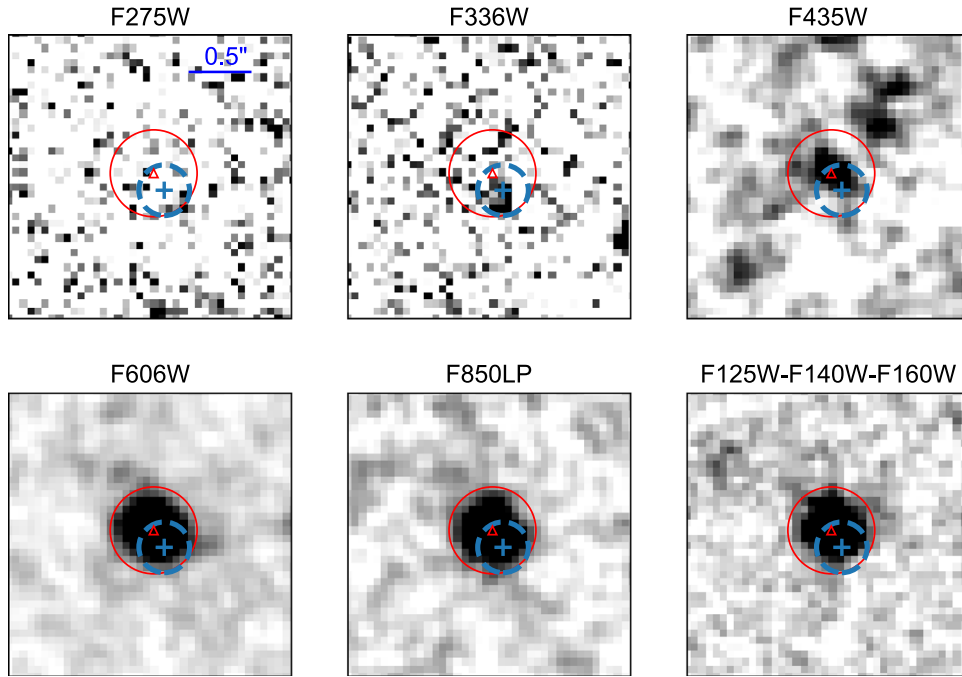
Figure 1. HST multiwavelength images of CDFS-6664 with a box size of $2\rlap{.}''4 \times 2\rlap{.}''4$. The center of the F336W band detection is marked by the red plus. The $0\rlap{.}''4$ aperture of the source detected by F336W band is indicated in each image with the blue dashed line. The red triangle on each panel indicates the center of the source measured from the F160W image. The red circle shows an aperture of $0\rlap{.}''7$ diameter, corresponding to a physical scale of ~ 5.0 kpc at $z = 3.797$.

and cMpc) to indicate the proper (comoving) distances. The AB magnitude system AB $= -2.5 \log(f/\mathrm{Jy}) + 8.9$) and a cosmology of Ω_{tot}, Ω_{M}, $\Omega_{\Lambda} = 1.0, 0.3, 0.7$ with $H_0 = 70$ km s^{-1} Mpc^{-1} are used.

2. Data

The LyC emitter candidate, named CDFS-6664, was selected from an emission line Lyman break galaxy (LBG) sample at $z \sim 3.5$, which includes a compilation of spectroscopic observations using near-infrared instruments on large ground telescopes (VLT SINFONI and Keck I MOSFIRE). A more detailed description of the sample can be found in our previous work (Yuan et al. 2019).

We use the publicly available images from the Hubble Deep UV Legacy Survey (HDUV, Oesch et al. 2018) at F275W and F336W bands with 5σ depths of 27.6 and 28.0 mag, respectively, in the GOODS-S field. In addition to the restframe UV data, we also use the 3D-HST images from F435W to F160W (Grogin et al. 2011; Koekemoer et al. 2011; Skelton et al. 2014) to analyze the escape fraction of the LyC photons. All these images are registered to the WFC3 mosaics based on their header WCS and re-binned to a $0\rlap{.}''06$ pix^{-1} scale. We show the images of CDFS-6664 from F275W to F160W bands in Figure 1. Visually, the source can be marginally seen in the F336W band at the lower right position relative to its F435W, F606W, and F160W detection. There is no confusion source nearby to contaminate the emission.

The source can be detected in the F336W band by SExtractor (Bertin & Arnouts 1996) with the same parameters used in the CANDELS "hot" mode (Guo et al. 2013). The position of the F336W detection is shown in Figure 1. The signal-to-noise ratio (S/N) is 7.9 for the isophotal measurement, 6.5 in an aperture of $0\rlap{.}''4$, and 5.0 in an aperture of $0\rlap{.}''7$. CDFS-6664 has an aperture magnitude of 27.9 ± 0.2 in the $0\rlap{.}''7$ aperture. We also run SExtractor in dual-image mode using an aperture of

$0\rlap{.}''7$. The detection image is a noise-equalized combination of the F125W, F140W, and F160W images. Following the method used by Skelton et al. (2014), we find that the total magnitude is 27.7 ± 0.2 after applying the aperture to total correction by a factor of $f_{\mathrm{F160W,total}}/f_{\mathrm{F160W,aper}}$. This total magnitude is used in the spectral energy distribution (SED) analysis in Section 3.

In fact, CDFS-6664 has already been included in the HDUV and Hubble Legacy Fields (HLF) catalogs (Oesch et al. 2018; Whitaker et al. 2019). The total magnitude at the F336W band is 27.7 ± 0.2 mag from the HDUV catalog and 27.5 ± 0.2 mag from HLF. Our measurement is closer to that given by the HDUV catalog. In the following, we take the total magnitude of CDFS-6664 in the F336W band as 27.7 ± 0.2 mag. This value corresponds to a flux of $3.0 \pm 0.6 \times 10^{-31}$ erg s^{-1} cm^{-2} Hz^{-1}.

We note that CDFS-6664 has not been detected by VIMOS U_V band (Nonino et al. 2009), whose depth is about 28.1 mag. According to the catalog data, we find that the completeness of the VIMOS U_V to detect the 5σ F336W sources is about 70%. The VIMOS U_V band probes wavelength slightly redder than the F336W band, but still well within the LyC domain at $z \approx 3.8$. A galaxy with similar redshift and magnitude, named *Ion1*, is detected with S/N ~ 6.6 in the U_V band (Vanzella et al. 2015). The fact that there is no such detection for CDFS-6664 poses doubts about the reliability of the F336W detection. However, the VIMOS U_V coverage within the CDFS field is not uniform. CDFS-6664 is coincidentally located in a gap region where the total exposure time is only $<80\%$ of that for *Ion1* (66,933 s versus 84,209 s) and about a half of the maximum.[3] Moreover, this galaxy is surrounded by several bright galaxies that elevate the level of the background, causing difficulty to detect faint sources. We show in Figure 2 that there

---

[3] According to the single-exposure images provided by ESO Science Archive (http://archive.eso.org/cms/html).
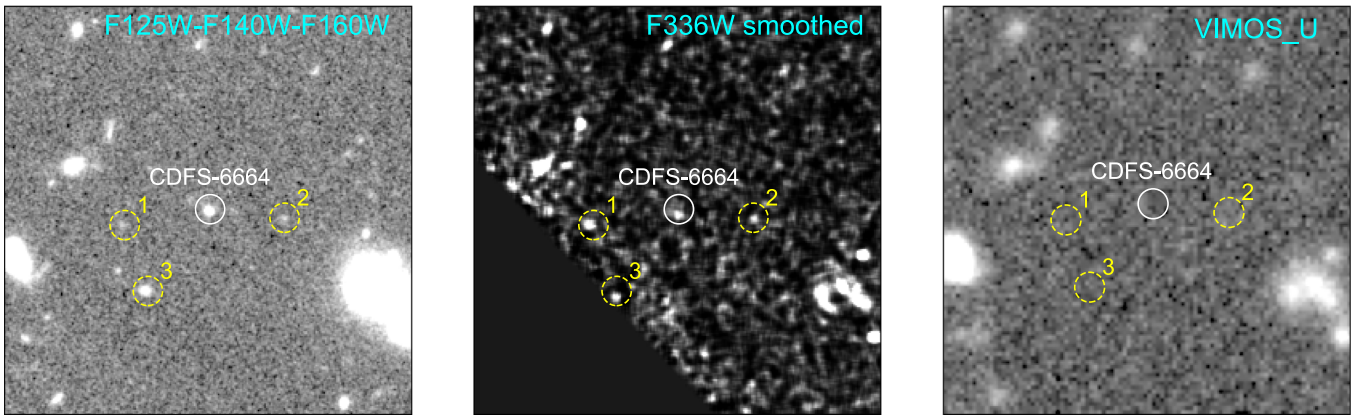
Figure 2. Galaxies that have been detected in the F336W band but not in the VIMOS U_V band. Left: the 3D-HST source detection image, which is a noise-equalized combination of the F125W, F140W, and F160W images. Middle: F336W image that has been smoothed with a Gaussian kernel with $\sigma = 0''3$. Right: VIMOS U_V image. The box size is $20'' \times 20''$.
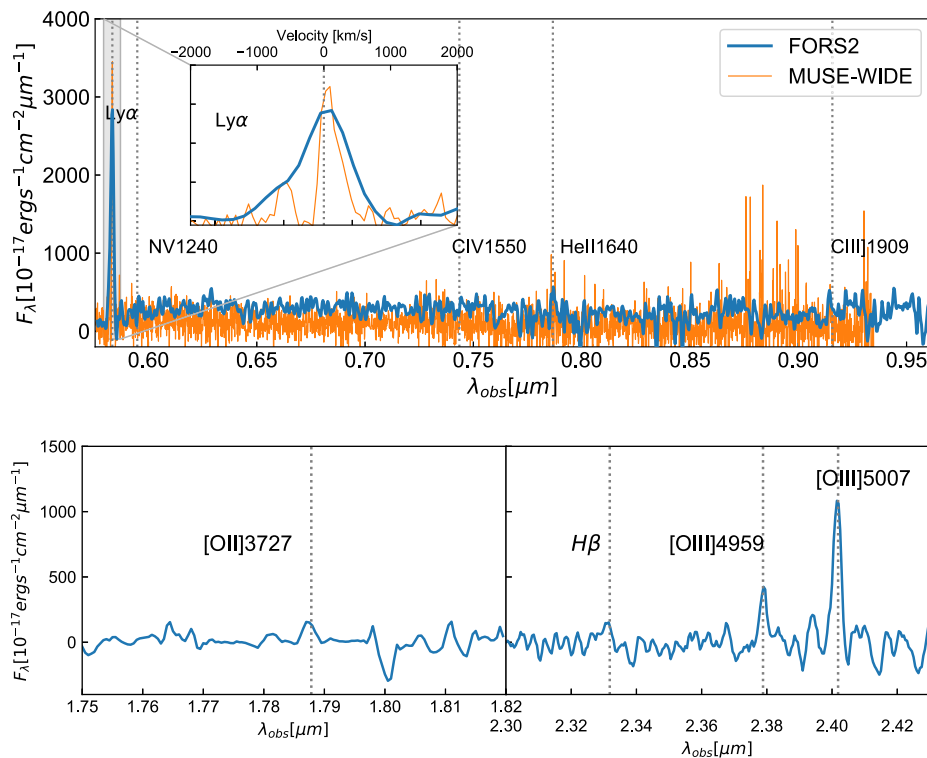

Figure 3. Upper panel: optical spectrum of CDFS-6664 from VLT/FORS2 observation by Vanzella et al. (2006) (thick blue line) and from MUSE-Wide observation by Urrutia et al. (2019) (thin orange line). Lower panel: near-infrared spectrum (smoothed) of CDFS-6664 from VLT/SINFONI observation by the AMAZE project (Maiolino et al. 2008). In both panels, the vertical dotted line marks the observed wavelength of each emission line based on the systemic redshift ($z = 3.797$, calculated from [O III]).

are about four galaxies (including CDFS-6664) that have been missed by the VIMOS U_V image in this region.

3. Spectroscopic and Photometric Properties

The optical spectrum by VLT/FORS2 observation (Vanzella et al. 2006) shows that this galaxy is also a Lyα emitter, with Lyα equivalent width $\sim 148 \pm 37$ Å (Figure 3). The spectral resolution of VLT/FORS2 ($R \sim 660$) is not high enough for us to carry out further analysis on the structure of the Lyα line. Fortunately, CDFS-6664 has also been observed by the MUSE-Wide survey (Urrutia et al. 2019). The spectrum is shallower than the VLT/FORS2 one but has a higher spectral resolution

($R \sim 3000$). The Lyα line shows double peaks. The blue and red peaks are offset from the systemic velocity by ~ -600 km s^{-1} and 100 km s^{-1}, respectively. The Lyα emission emerging at the systemic velocity is an important tracer for LyC leakers because it indicates clumpy, multiphase systems with nonunity covering fractions (Naidu et al. 2021). For CDFS-6664, the central escape fraction of Lyα emission within ± 100 km s^{-1} of the systemic velocity f_{cen} is about 28%, consistent with the LyC leakers with $f_{esc} > 20\%$ (e.g., Vanzella et al. 2020; Naidu et al. 2021).

High-ionization emission lines like N V 1240 and C IV 1550 have not been detected at more than the 3σ level, while the
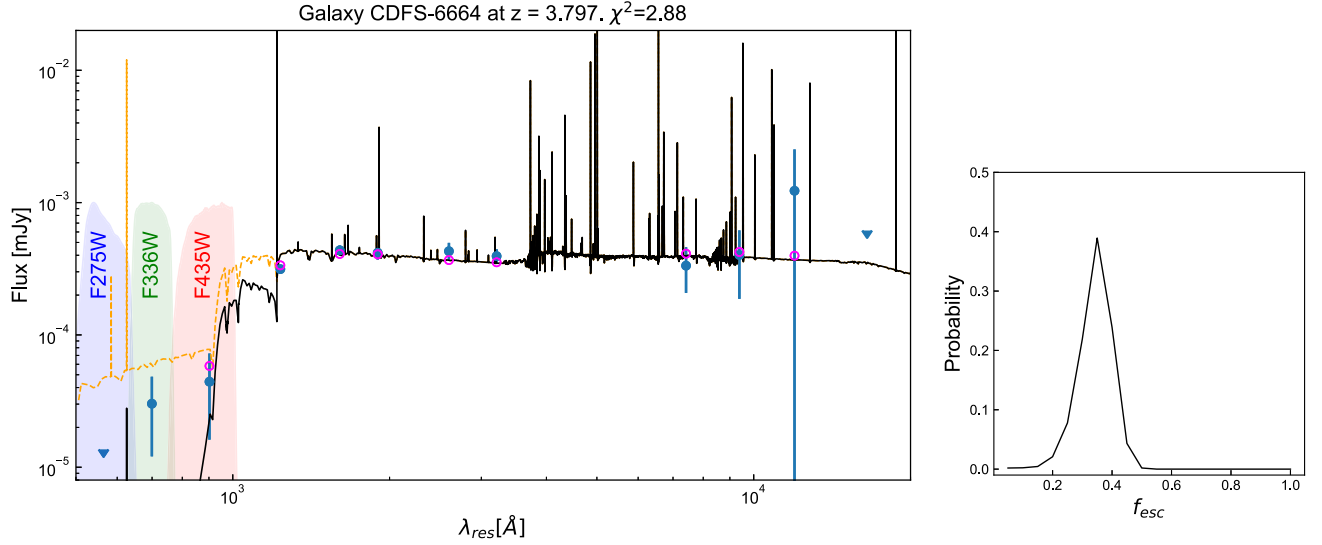
Figure 4. SED fitting for CDFS-6664. Left panel: the blue dots are the observed broadband fluxes. The down triangles are the observed upper limits. The black solid line is the spectrum of the best-fit model. The magenta circles are the broadband fluxes estimated from the best-fit model. The spectrum with no IGM absorption is shown as the orange dashed line. The filter response curves of F275W, F336W, and F435W are shown as blue, green, and red shaded areas, respectively. Right panel: the probability density distribution of $f_{\rm esc}$.

He II 1640 and C III] 1909 lines are detected. Based on the FORS2 spectrum, the He II 1640 and C III] 1909 are estimated as $5.9 \pm 1.4 \times 10^{-18}$ and $5.4 \pm 1.4 \times 10^{-18}$ erg s^{-1} cm^{-2}, respectively. From the ratio of C III] 1909/He II 1640 ($\sim$0.9 $\pm$ 0.3), and following Feltre et al. (2016), this source is classified as a star-forming galaxy lying in the same region occupied by low-metallicity galaxies of Stark et al. (2014).

CDFS-6664 has also been observed in the near-infrared band using VLT/SINFONI by the AMAZE project (Maiolino et al. 2008). The near-infrared spectrum shows that this galaxy has [O III]/[O II] $\sim$ 10 (Figure 3). Both the large oxygen ratio and the strong [O III]4959,5007 emission lines fit the profile predicted by the photon ionization models for an LyC candidate emitter (Jaskot & Oey 2014; Nakajima & Ouchi 2014).

We then analyze the panchromatic SED of CDFS-6664 from UV to midinfrared bands using the broadband data from HST and Spitzer observations. We also include the flux of [O II], Hβ, [O III]4959, and [O III]5007 in the fitting to provide more constraints on the stellar mass and SFR (Yuan et al. 2019). In the above analysis, we use the total magnitude in the SED fitting to keep the measurements of the continuum and the emission lines consistent.

We use Code Investigating GALaxy Emission (CIGALE, Burgarella et al. 2005; Noll et al. 2009; Boquien et al. 2019) to fit the SED with models of stars, gas, and dust. The SED of CDFS-6664 can be fitted well assuming a delayed star formation history (Figure 4). The most significant discrepancy between the data and model comes from the UV bands because the average IGM model (Meiksin 2006) used in CIGALE is not consistent with the observation. We discuss the IGM effect in Section 4.

The results of SED fitting show that CDFS-6664 is a low-mass galaxy with $\log(M_*/M_\odot) = 9.15 \pm 0.15$ and star formation rate of $52.1 \pm 4.9\,M_\odot$ yr^{-1}. The stellar population of this galaxy is quite young, with an average age of 0.05 ± 0.01 Gyr.

The dust attenuation for this galaxy is quite low, with $E(B-V)_s = 0.10 \pm 0.05$.

CIGALE also obtains an escape fraction based on the SED. The fitting result gives $f_{\rm esc} = 0.38 \pm 0.07$. Examining the shape of the probability density function (Figure 4), we find the parameter $f_{\rm esc}$ is well constrained in the fitting. The degeneracy between $f_{\rm esc}$ and IGM transmission is broken by the constraints introduced from the emission line data, assuming

$$L_{\rm H\beta}(f_{\rm esc}) = L_{\rm H\beta}(0) \times \frac{1 - f_{\rm esc}}{1 + 0.6 f_{\rm esc}} \qquad (1)$$

where $L_{\rm H\beta}$ is the luminosity of the Hβ line emission (Inoue 2011). The electron temperature T_e is assumed to be 10^4 K (Inoue 2011; Boquien et al. 2019). The ionization parameter U is assumed to have $\log U = -2.5$, corresponding to $\log q_{\rm ion}/{\rm cm\ s}^{-1} = 8.0$, consistent with the value for local LyC leakers (Nakajima & Ouchi 2014).

4. Discussion

4.1. LyC Morphology

The spatially resolved images of HST enable us to analyze the morphology of CDFS-6664. Using GALFIT to fit the image of the F160W band, we found that the profile of the galaxy can be well described by a single Sérsic component, with a reduced χ^2 of 1.038. The Sérsic index of the galaxy is 0.83, suggesting a disk-like morphology. CDFS-6664 has a physical half-light radius of 1.3 kpc, which is more extended than previously found LyC emitters at $z > 3$, such as *Ion1* (Vanzella et al. 2015; Ji et al. 2020, $z = 3.795$), *Ion2* (de Barros et al. 2016; Vanzella et al. 2016, $z = 3.2$), J0121+0025 (Marques-Chaves et al. 2021, $z = 3.24$).

Comparing the F336W image with other bands, we find that the LyC emitting region is confined to a small area that deviates from the center of the galaxy. The images of CDFS-6664 of other bands show no sign of any possible low-redshift interloper at this position. Similar offsets have been found in

Ion1, which is at a redshift very close to CDFS-6664, and several other high-redshift galaxies (e.g., Micheva et al. 2017). The deviation from the center of the LyC emission may imply a clumpy distribution of the ISM caused by the strong star-forming activities in this galaxy.

The deviated LyC emission also implies that the normal stacking method may underestimate the escape fraction of the LyC photons because the stacking is always done by matching the centers of different galaxies. If LyC photons are not from the center, the signals cannot be enhanced by such stacking.

4.2. The Source of LyC Photons

We analyze the photometric and spectroscopic data of CDFS-6664 to investigate the possibility of an active galactic nucleus (AGN) contribution. We summarize the following aspects suggesting that the source is more likely to be a stellar origin:

First, CDFS-6664 is in the sample of the AMAZE project (Maiolino et al. 2008; Troncoso et al. 2014), in which LBGs that host AGNs are discarded based on the UV/optical spectra, X-ray data or the MIPS 24 μm fluxes. Furthermore, as mentioned in Section 3, the line ratio of C III] 1909/He II 1640 ($\sim$0.6) shows that this source is located in the same region occupied by star-forming galaxies. Considering the facts that the UV/optical spectra cannot remove type-2 AGN, and that X-ray/MIPS 24 μm are both redshift-dependent so that they may miss a low-luminosity AGN, these pieces of evidence cannot rule out the possibility of an AGN origin for the LyC photons. Nevertheless, these data show that the probability of AGN contributing to the LyC photons for this source is quite low.

Second, the SED fitting shows that the UV spectral slope β is -2.25 ± 0.03. This slope is not extremely steep but indicates a rather blue UV color. Therefore, it is likely that the LyC photons are generated from the massive young stars in UV bright clumps.

Finally, from the morphological fittings of the profiles of F160W and F435W images using GALFIT, we find that the morphology of CDFS-6664 is more close to disk-like. The off-central morphology in the F336W band resembles the extended UV emission found in the star-forming regions of the nearby galaxies, supporting the scenario that the LyC photons are coming from the star-forming regions. The disk-like and clumpy morphology further reduces the possibility that it is an AGN dominant source.

4.3. LyC Escape Fraction and IGM Transmission

The escape fraction of a galaxy can be calculated by the following equation:

$$f_{\rm esc} = \frac{(L_{1500}/L_{800})_{\rm int}}{(L_{1500}/L_{800})_{\rm obs}} \times T_{\rm IGM, F336W}^{-1} \times 10^{-0.4\,A_{1500}}, \quad (2)$$

where L_{1500} and L_{800} are the nonionizing ($\lambda_{\rm rest} = 1500$ Å) and ionizing ($\lambda_{\rm rest} = 800$ Å) luminosity from the galaxy, respectively. $T_{\rm IGM, F336W}^{-1}$ is the IGM transmission at the F336W band. A_{1500} is the attenuation at 1500 Å. Here we assume that the dust affects only the nonionizing UV (i.e., $A_{800} = 0$) (see e.g., Steidel et al. 2018).

In previous works, by assuming the transmission of the IGM and the intrinsic ratio of the UV to LyC photons $((L_{1500}/L_{800})_{\rm int})$, one can estimate the value of $f_{\rm esc}$. In this
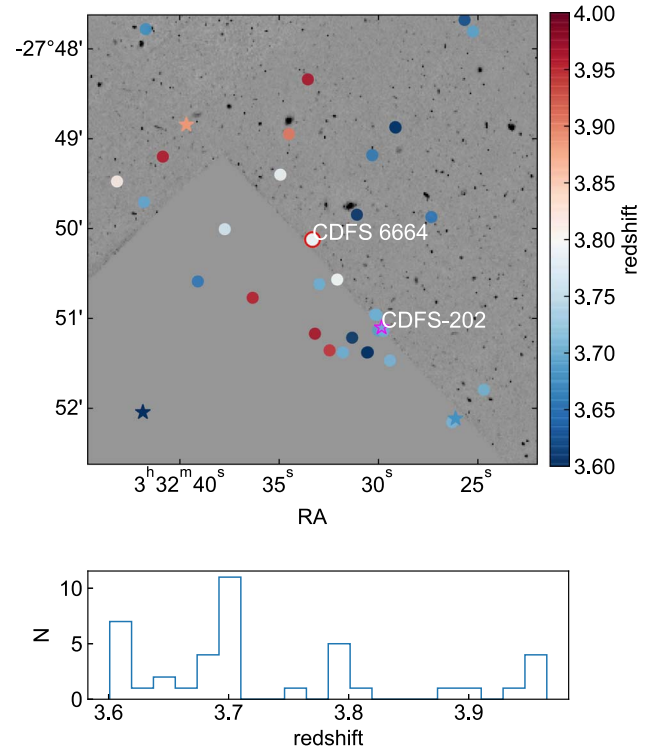

Figure 5. Upper panel: spatial distribution of CDFS-6664 and CDFS-202 overplotted on the F336W images ($5' \times 5'$). The colored dots and stars show the galaxies and quasars with spectroscopically confirmed redshifts $3.6 \leqslant z \leqslant 4.0$, respectively. Lower panel: redshift distribution of the galaxies shown in the upper panel.

work, instead of using the assumption on the IGM transmission, we estimate the $f_{\rm esc}$ by assuming the ISM properties. As mentioned in Section 3, the SED fitting provide constraints on the $f_{\rm esc}$ by the nebular radiative transfer model and obtain the value to be $\sim$0.4. The result is also consistent with the $f_{\rm esc}$ derived from the [O III]/[O II] ratio using the relation given by Nakajima & Ouchi (2014) or Nakajima et al. (2020). This is not surprising because both of the methods are based on the nebular models.

Adopting the value $f_{\rm esc}$ as 40%, the $T_{\rm IGM}$ is estimated to be $\sim$60% from Equation (2). Even if we use the 99th percentile value of the $f_{\rm esc}$ probability density distribution ($\sim$45%), the $T_{\rm IGM}$ is about $\sim$53%, which is higher than the 99th percentile of the simulated IGM transmission value (about 35%) at such a redshift based on the results of Steidel et al. (2018). As also shown in the SED fitting, the average IGM model given by Meiksin (2006) cannot fit the observed fluxes for F435W and F336W bands. The discrepancy can be explained by the extremely stochastic property of the IGM (e.g., Inoue & Iwata 2008). Recent works also find that the mean IGM transmission may not suitable for LyC emitters (Bassett et al. 2021; Prichard et al. 2021).

In addition to the inhomogeneous nature of the IGM, we consider the possibility that a foreground quasar close to the sightline may ionize its surrounding IGM and open a path for the LyC photons of CDFS-6664 to the observers. We check the quasar catalog and find that the famous type-2 quasar, CDFS-202 (Norman et al. 2002), is close to the sightline of CDFS-6664, with a project separation of 0.5 pMpc ($1.'2$, Figure 5). CDFS-202 is located at redshift 3.71. The line-of-sight distance to CDFS-6664 is about 64.9 cMpc. Previous works show that

luminous quasars can photoevaporate optically thick absorbers within a ∼1 pMpc radius or so (e.g., Hennawi & Prochaska 2007). Therefore, it is quite possible that the ionization bubble of CDFS-202 affect the IGM on the sightline of the CDFS-6664 and enhances the transmission of LyC photons.

We also plot the sources with known spectroscopic redshift higher than 3.6 near CDFS-6664. The redshift distribution shows a narrow peak at $z = 3.7$, indicating a clustering of sources at this redshift, as shown in Figure 5. These sources may present extra ionizing background, further increase the transmission of the IGM at this region (e.g., Adelberger et al. 2003).

5. Summary

This work reports the discovery of a candidate LyC emission from the LBG, CDFS-6664, at $z = 3.797$. The galaxy has an [O III]/[O II] value of about 10 and an asymmetric Lyα line profile, both indicating possible leakage of LyC photons. Based on the HDUV F336W band image, we found a detection at 27.9 ± 0.2 mag in an aperture of $0\farcs7$, corresponding to 650–770 Å rest frame.

We further investigate the properties of this galaxy using the spectroscopic and photometric data. The data show the AGN contribution to the LyC emission is negligible. We derived from the SED fitting that the average age of the stellar populations is about 50 Myr, and the SFR is $52.1 \pm 4.9\, M_\odot\, \mathrm{yr}^{-1}$. These results show that the source of the LyC photons is more likely to be the massive young stars.

We break the degeneracy between the escape fraction and the IGM transmission by constraining the escape fraction using the nebular model and the observed Hβ emission. In this way, the escape fraction is estimated to be $38\% \pm 7\%$. Consequently, the IGM transmission for this galaxy is about 60%, exceeding the 99th percentile transmission (35%) obtained by the simulation at this redshift.

The unusually high transmission of the IGM along the line of sight of CDFS-6664 can be explained by the stochastic nature of the IGM. Morever, the foreground ionizing sources may increase the transmission on the sightline. Specifically, we found that the quasar CDFS-202 is close enough to the sightline of CDFS-6664 (0.5 pMpc projected separation) to ionize the foreground IGM and increase the free path for the LyC photons. Whether LyC emitters and quasars are spatially correlated requires further investigation.

Additionally, the LyC emission of CDFS-6664 is offset from the galaxy center, indicating a clumpy distribution of the ISM in the galaxy. The spatially offset LyC emission implies that the escape fraction can be higher in some regions of galaxies than estimated from the entire galaxy. If the spatially offset LyC emission is normal in high-redshift galaxies, the commonly adopted stacking method by previous works may underestimate the escape fraction of LyC photons.

In addition to CDFS-6664, we have also detected a few suspicious off-center LyC signals at the F336W band for the emission line galaxies in our sample. However, the current depth of the UV surveys (∼28 mag) is not able to confirm these detections. Further investigation of these sources requires deeper imaging in UV bands. In particular, the extreme deep field project with the Multi-channel Imager instrument carried by the Chinese Space Station Telescope plan to reach the depth of ≳29 mag at its near-UV band (Yuan et al. 2022). The data

product will provide us an unprecedented chance to investigate the LyC emitters statistically.

ORCID iDs

Fang-Ting Yuan ⓘ https://orcid.org/0000-0001-6763-5869
Zhen-Ya Zheng ⓘ https://orcid.org/0000-0002-9634-2923
P. T. Rahna ⓘ https://orcid.org/0000-0002-5864-7195

References

Adelberger, K. L., Steidel, C. C., Shapley, A. E., & Pettini, M. 2003, ApJ, 584, 45
Alexandroff, R. M., Heckman, T. M., Borthakur, S., Overzier, R., & Leitherer, C. 2015, ApJ, 810, 104
Bassett, R., Ryan-Weber, E. V., Cooke, J., et al. 2021, MNRAS, 502, 108
Bertin, E., & Arnouts, S. 1996, A&AS, 117, 393
Bian, F., Fan, X., McGreer, I., Cai, Z., & Jiang, L. 2017, ApJL, 837, L12
Boquien, M., Burgarella, D., Roehlly, Y., et al. 2019, A&A, 622, A103
Burgarella, D., Buat, V., & Iglesias-Páramo, J. 2005, MNRAS, 360, 1413
Dayal, P., & Ferrara, A. 2018, PhR, 780, 1
Dayal, P., Volonteri, M., Choudhury, T. R., et al. 2020, MNRAS, 495, 3065
de Barros, S., Vanzella, E., Amorín, R., et al. 2016, A&A, 585, A51
Feltre, A., Charlot, S., & Gutkin, J. 2016, MNRAS, 456, 3354
Fletcher, T. J., Tang, M., Robertson, B. E., et al. 2019, ApJ, 878, 87
Grazian, A., Giallongo, E., Paris, D., et al. 2017, A&A, 602, A18
Grogin, N. A., Kocevski, D. D., Faber, S. M., et al. 2011, ApJS, 197, 35
Guo, Y., Ferguson, H. C., Giavalisco, M., et al. 2013, ApJS, 207, 24
Heckman, T. M., Borthakur, S., Overzier, R., et al. 2011, ApJ, 730, 5
Hennawi, J. F., & Prochaska, J. X. 2007, ApJ, 655, 735
Hopkins, P. F., Richards, G. T., & Hernquist, L. 2007, ApJ, 654, 731
Inoue, A. K. 2011, MNRAS, 415, 2920
Inoue, A. K., & Iwata, I. 2008, MNRAS, 387, 1681
Izotov, Y. I., Worseck, G., Schaerer, D., et al. 2018, MNRAS, 478, 4851
Jaskot, A. E., & Oey, M. S. 2014, ApJL, 791, L19
Ji, Z., Giavalisco, M., Vanzella, E., et al. 2020, ApJ, 888, 109
Koekemoer, A. M., Faber, S. M., Ferguson, H. C., et al. 2011, ApJS, 197, 36
Madau, P., & Dickinson, M. 2014, ARA&A, 52, 415
Maiolino, R., Nagao, T., Grazian, A., et al. 2008, A&A, 488, 463
Marques-Chaves, R., Schaerer, D., Álvarez-Márquez, J., et al. 2021, MNRAS, 507, 524

Meiksin, A. 2006, MNRAS, 365, 807
Micheva, G., Iwata, I., Inoue, A. K., et al. 2017, MNRAS, 465, 316
Mostardi, R. E., Shapley, A. E., Steidel, C. C., et al. 2015, ApJ, 810, 107
Naidu, R. P., Matthee, J., Oesch, P. A., et al. 2021, arXiv:2110.11961
Nakajima, K., Ellis, R. S., Robertson, B. E., Tang, M., & Stark, D. P. 2020,
    ApJ, 889, 161
Nakajima, K., & Ouchi, M. 2014, MNRAS, 442, 900
Noll, S., Burgarella, D., Giovannoli, E., et al. 2009, A&A, 507, 1793
Nonino, M., Dickinson, M., Rosati, P., et al. 2009, ApJS, 183, 244
Norman, C., Hasinger, G., Giacconi, R., et al. 2002, ApJ, 571, 218
Oesch, P. A., Montes, M., Reddy, N., et al. 2018, ApJS, 237, 12
Prichard, L. J., Rafelski, M., Cooke, J., et al. 2021, arXiv:2110.06945
Saha, K., Tandon, S. N., Simmonds, C., et al. 2020, NatAs, 4, 1185
Shapley, A. E., Steidel, C. C., Strom, A. L., et al. 2016, ApJL, 826, L24
Siana, B., Shapley, A. E., Kulas, K. R., et al. 2015, ApJ, 804, 17

Skelton, R. E., Whitaker, K. E., Momcheva, I. G., et al. 2014, ApJS, 214, 24
Stark, D. P., Richard, J., Siana, B., et al. 2014, MNRAS, 445, 3200
Steidel, C. C., Bogosavljević, M., Shapley, A. E., et al. 2018, ApJ, 869, 123
Steidel, C. C., Pettini, M., & Adelberger, K. L. 2001, ApJ, 546, 665
Troncoso, P., Maiolino, R., Sommariva, V., et al. 2014, A&A, 563, A58
Urrutia, T., Wisotzki, L., Kerutt, J., et al. 2019, A&A, 624, A141
Vanzella, E., Caminha, G. B., Calura, F., et al. 2020, MNRAS, 491, 1093
Vanzella, E., Cristiani, S., Dickinson, M., et al. 2006, A&A, 454, 423
Vanzella, E., de Barros, S., Castellano, M., et al. 2015, A&A, 576, A116
Vanzella, E., de Barros, S., Vasei, K., et al. 2016, ApJ, 825, 41
Verhamme, A., Orlitová, I., Schaerer, D., & Hayes, M. 2015, A&A, 578, A7
Whitaker, K. E., Ashas, M., Illingworth, G., et al. 2019, ApJS, 244, 16
Yuan, F.-T., Burgarella, D., Corre, D., et al. 2019, A&A, 631, A123
Yuan, F.-T., Zheng, Z., Rahna, P. T., Lin, R., & Zhu, S. 2022, SSPMA, 52,
    229801